Numerical simulation of self-propelled motion of a torus rotating about its centerline in a viscous incompressible fluid

N.P.Moshkin
Institute of Science, Suranaree University of Technology,
Nakhon ratchasima, 30000, Thailand
e-mail: nikolay.moshkin@gamil.com

P. Suwannasri
Department of Mathematics Statistics and Computer,
Faculty of Science, Ubon Ratchathani University, Ubon Ratchathani, 34190, Thailand

In the present work, the problem of the motion of self-propelled torus in a viscous incompressible fluid is investigated numerically. The surface of torus rotates with constant velocity around its centerline. The rotating boundary of a torus generates inertia in the surrounding fluid. The outer and inner portions produce inertia in opposite directions. There are two self-motion regimes. In one of them, the torus moves in the direction of the inner surface motion due to the larger production of inertia by the outer portion of the torus boundary. The direction of propulsion is the same as in the case of zero Reynolds number. In another one the torus moves in opposite direction due to the high momentum flux associated with the jet of fluid expelled from the hole. The drag coefficients and flow patterns are analyzed at Reynolds numbers $Re = 20, 30, 40$, (Reynolds number defined by velocity of uniform stream and smaller diameter of torus), the aspect ratios $Ar = 2, 3$, (aspect ratio is defined as ratio of torus diameter to cross-section diameter of torus), and a range of rotational rate $-4.5 \le \alpha \le 2.5$ (α is defined as ratio of tangential tank-treading motion of torus surface to the uniform far-field velocity).

1. Introduction

The flow around self-propelled body could be quite different from that of a passively towed body. Flow past towed bluff-body have been of interest to researchers for many decades. To realize a self-propelled motion a body must have its own source of energy to overcome the energy spent against the drag force. In pure motion by self-propulsion the total net force and torque, external to the system body-fluid, acting on the body are zero. Although the problem of fluid flow past delf-propelled body originates in nature and its of practical importance, the number of works concerning it is limited. The review of the work on this research can be found in [1, 2] and therein literature references.

The hydrodynamics of a torus is important because it has the simplest geometry which can describe self-propelled motion of microorganisms. Purcell [3] suggested considering a rotational torus as a toroidal swimmer. The papers [2, 4]address the hydrodynamics of torus rotating about its centerline in the zero Reynolds number. Both papers demonstrate that torus moves in the direction of the inside surface motion. The mechanism of propulsion is based on the difference in viscous friction to the rotation of the inner (i.e. in the hall) and outer parts of the torus surface. However, it is pointed out without detailed discussion in [2] that there is a reversal propulsion direction at a higher speed of torus rotation. The motion happened due to the inertia of the jet expelled by the inner surface rotation prevails over production of inertia by the outer portion of torus boundary.

In the present work the hydrodynamics of torus, rotating about its centerline at low nonzero Reynolds number is addressed. The two direction of self-motion are compared and analyzed.

2. Governing equations

Assuming the flow remains axisymmetric for all time, *makes the toroidal coordinate system attached to the torus*:

$$x = \frac{c \sinh \eta \cos \varphi}{\cosh \eta - \cos \xi}, \qquad y = \frac{c \sinh \eta \sin \varphi}{\cosh \eta - \cos \xi}, \qquad z = \frac{c \sin \xi}{\cosh \eta - \cos \xi}, \tag{1}$$

where $\xi \in (0, 2\pi]$, $\eta \in (-\infty, \infty)$ and $\varphi \in [0, 2\pi)$, $c > 0$ is the characteristic length, the natural choice. The surface $\eta = \eta_0$ defines a torus, $z^2 + (r - c \coth \eta_0)^2 = c^2 \mathrm{csch}^2 \eta_0$, and the surface $\xi = \xi_0$ define a spherical bowl, $(z - c \cot \eta_0)^2 + r^2 = c^2 \csc^2 \xi_0$, where $r^2 = \sqrt{x^2 + y^2} = \dfrac{c \sinh \eta}{\cosh \eta - \cos \xi}$. Figure 1 shows the torus with radius $b = c \coth \eta$ and the circular cross-section radius $a = c\, \mathrm{csch} \eta_0$. If a and b are given, one can find c and η_0 as the following

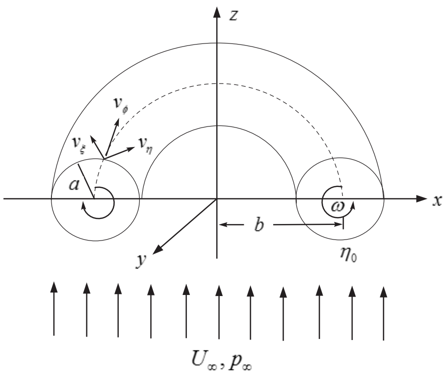

Fig. 1. Sketch of the geometry of the torus.

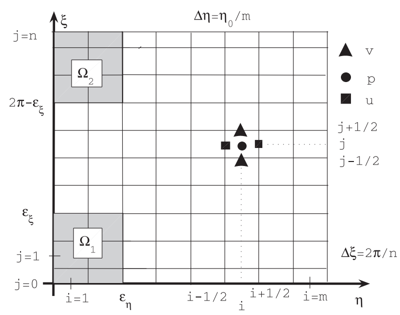

Fig. 2. Staggered arrangement of u,v and p.

$$c = \sqrt{b^2 - a^2}, \qquad \eta_0 = \ln \left(\left(\frac{b}{a} \right) - \sqrt{\left(\frac{b}{a} \right)^2 - 1} \right).$$

The torus geometry is described by the aspect ratio parameter $Ar = b/a$. In terms of the toroidal coordinates and the assumption of axisymmetry, the governing Navier-Stokes equations in dimensionless form are given by

$$\begin{aligned}
&\frac{\partial v_\xi}{\partial t}+\frac{1}{h}\left(v_\xi\frac{\partial v_\xi}{\partial \xi}+v_\eta\frac{\partial v_\xi}{\partial \eta}\right)+\frac{1}{c}\left[v_\eta^2\sin\xi-v_\xi v_\eta\sinh\eta\right]=-\frac{1}{h}\frac{\partial p}{\partial \xi}\\
&+\frac{2}{Re}\left[\frac{1}{h^2}\left(\frac{\partial^2 v_\xi}{\partial \xi^2}+\frac{\partial^2 v_\xi}{\partial \eta^2}\right)-\frac{1}{ch}\left(\sin\xi\frac{\partial v_\xi}{\partial \xi}+2\sinh\eta\frac{\partial v_\eta}{\partial \xi}-2\sin\xi\frac{\partial v_\eta}{\partial \eta}\right)\right.\\
&+\left(\frac{\coth\eta}{h^2}-\frac{1}{ch}\sinh\eta\right)\frac{\partial v_\xi}{\partial \eta}+\left(\frac{\sin\xi}{c^2\sinh\eta}\left((2-2\cosh\eta\cos\xi)+\sinh^2\eta\right)\right)v_\eta\\
&\left.+\left(\frac{1}{ch}\cosh\eta-\frac{2}{c^2}\left(\sin^2\xi+\sinh^2\eta\right)+\frac{1}{c^2}\left(\cosh\eta\cos\xi-1\right)\right)v_\xi\right],
\end{aligned}\tag{2}$$

$$\begin{aligned}
&\frac{\partial v_\eta}{\partial t}+\frac{1}{h}\left(v_\xi\frac{\partial v_\eta}{\partial \xi}+v_\eta\frac{\partial v_\eta}{\partial \eta}\right)+\frac{1}{c}\left[v_\xi^2\sinh\eta-v_\xi v_\eta\sin\xi\right]=-\frac{1}{h}\frac{\partial p}{\partial \eta}\\
&+\frac{2}{Re}\left[\frac{1}{h^2}\left(\frac{\partial^2 v_\eta}{\partial \xi^2}+\frac{\partial^2 v_\eta}{\partial \eta^2}\right)-\frac{1}{ch}\left(\sin\xi\frac{\partial v_\eta}{\partial \xi}-2\sinh\eta\frac{\partial v_\xi}{\partial \xi}+2\sin\xi\frac{\partial v_\xi}{\partial \eta}\right)\right.\\
&+\left(\frac{\coth\eta}{h^2}-\frac{\sinh\eta}{ch}\right)\frac{\partial v_\eta}{\partial \eta}+\left(\frac{\cosh\eta}{ch}-\frac{2}{c^2}\left(\sin^2\xi+\sinh^2\eta\right)\right)v_\eta\\
&\left.+\left(\frac{1}{c^2}\left(\sin^2\xi+(\cosh\eta\cos\xi-1)+\frac{(1-\cosh\eta\cos\xi)^2}{\sinh^2\eta}\right)\right)v_\eta-\frac{\sin\xi\sinh\eta}{c^2}v_\xi\right],
\end{aligned}\tag{3}$$

$$\frac{1}{h}\left(\frac{\partial v_\xi}{\partial \xi}+\frac{\partial v_\eta}{\partial \eta}\right)-\frac{2h\sin\xi}{c}v_\xi+\left(\coth\eta-\frac{2h\sinh\eta}{c}\right)v_\eta=0,\tag{4}$$

where p is the pressure, v_ξ and v_η are the velocity components in ξ and η directions, respectively, and $h=c/(\cosh\eta-\cos\xi)$. The velocities are non dimensionalized with the free stream velocity U_∞, all lengths are non dimensionalized with the radius a and the pressure by ρU_∞^2. Here Re denotes the Reynolds number defined by $Re=\dfrac{2U_\infty a}{\nu}$, where ν is the kinematic viscosity coefficient. Boundary conditions for v_ξ and v_η include the no-slip and impermeability conditions

$$v_\xi=\alpha,\quad v_\eta=0,\quad \xi\in(0,2\pi],\ \eta=\eta_0,\tag{5}$$

where $\alpha=(a\omega)/U_\infty$ is the nondimensional rotational velocity at the surface, the periodicity conditions

$$v_\xi(\xi,\eta)=v_\xi(\xi+2\pi,\eta),\ v_\eta(\xi,\eta)=v_\eta(\xi+2\pi,\eta),\ p(\xi,\eta)=p(\xi+2\pi,\eta),\tag{6}$$

and the far-field condition

$$\mathbf{v}=(v_r,v_z)=(0,1),\quad p=\frac{p_\infty}{\rho U_\infty^2}\ \text{ as }\ r^2+z^2\to\infty.\tag{7}$$

Here, v_r and v_z are the components of the velocity vector in the cylindrical coordinate system with

$$\begin{aligned}
v_\xi&=\left(-\frac{h}{a}\sinh\eta\sin\xi\right)v_r+\left(\frac{h}{a}(\cosh\eta\cos\xi-1)\right)v_z\\
v_\eta&=\left(-\frac{h}{a}(\cosh\eta\cos\xi-1)\right)v_r-\left(\frac{h}{a}\sinh\eta\sin\xi\right)v_z.
\end{aligned}\tag{8}$$

On the axis of symmetry $r=0$ the velocity components and pressure satisfy the following conditions

$$\frac{\partial v_\xi}{\partial \eta}=0,\ v_\eta=0\ \text{and}\ \frac{\partial p}{\partial \eta}=0.\tag{9}$$

The two most important hydrodynamic characteristics of the flow around the body are the net force and angular momentum. The net force is decomposed into components F_L and F_D perpendicular and parallel to the flow direction. The net torque and F_L are equal to zero due to the symmetry of the flow. The drag coefficient is defined as $C_D = \dfrac{F_D}{0.5\rho A_{frontal} U_\infty^2}$, where ρ and $A_{frontal}$ are the fluid density and the projected frontal area of the body, respectively. The drag coefficient comprises a pressure drag coefficient and a viscous drag coefficient, *i.e.* $C_D = C_{D_p} + C_{D_f}$. They are defined as

$$C_{D_p} = -\frac{1}{2ab\pi\rho U_\infty^2}\int_0^{2\pi}\int_0^{2\pi} p\mathbf{n}\cdot\mathbf{i}_z h^2 \sinh\eta_0 d\phi d\xi = -\frac{\sinh^2\eta_0}{b}\int_0^{2\pi} p\frac{\sin\xi}{(\cosh\eta_0-\cos\xi)}h^2 d\xi,$$

$$C_{D_f} = -\frac{1}{2ab\pi\rho U_\infty^2}\int_0^{2\pi}\int_0^{2\pi} \mu\left(\mathbf{n}\times\boldsymbol{\omega}\right)\cdot\mathbf{i}_z h^2 \sinh\eta_0 d\phi d\xi = -\frac{\sinh^2\eta_0}{b}\int_0^{2\pi} \frac{2\omega\left(\cosh\eta_0-1\right)}{Re\left(\cosh\eta_0-\cos\xi\right)}h d\xi,$$

where $\mathbf{i}_r$ and $\mathbf{i}_z$ are the unit vectors in the r and z axes directions, respectively. The vorticity ω is defined by the following equation $\omega = \dfrac{1}{h^3\sinh\eta_0}\left(\dfrac{\partial}{\partial\xi}\left(hv_\eta\right) - \dfrac{\partial}{\partial\eta}\left(hv_\xi\right)\right)$.

3. Numerical solution method

In the case of steady flow, time in Equations (2) and (3) can be considered as an artificial (iterative) parameter. A staggered arrangement of the variables on a uniform grid is used. A two-step time-split projection method is utilized to advance the flow field. First, the velocity components are advanced from time level "n" to an intermediate level "*" by solving Equations (2) and (3) explicitly without the pressure term. In the advection-diffusion step, the spatial derivatives are approximated by the central finite differences. One side finite differences are utilized near boundaries due to the staggered arrangement of variables. Then the Poisson equation for the pressure is solved fully implicitly by the method of stabilizing correction (see Yanenko [5]). The equation for pressure is derived by using the mass conservation requirement for each computational cell. Once the pressure is updated, the final level is computed with a pressure-correction step. Figure 2 shows the computational domain, sketch of the grid, and location of the unknowns. Far-field boundary conditions (7) are shifted on the boundary of domains Ω_1 and Ω_2 which are defined as

$$\Omega_1 = \left\{(\xi,\eta)\ |\ 0\le\xi\le\varepsilon_\xi, 0\le\eta\le\varepsilon_\eta\right\},\ \Omega_2 = \left\{(\xi,\eta)\ |\ 2\pi-\varepsilon_\xi\le\xi\le 2\pi, 0\le\eta\le\varepsilon_\eta\right\},$$

where $\varepsilon_\eta = K\triangle_\eta$ and $\varepsilon_\xi = M\triangle_\xi$, K and M are integer numbers, and $\triangle_\eta$ and $\triangle_\xi$ are the size of computational cell in the η and ξ directions, respectively. In the physical space (x, y, z) the boundaries of domains Ω_1 and Ω_2 are located sufficiently far from the torus and these boundaries are the coordinate surfaces that are convenient for the implementation of a finite difference method.

4. Results

The characteristics of flow past a torus rotating about its centerline at the Reynolds numbers $Re = 20, 30$, and 40 with a rate of rotation of $-4.5\le\alpha\le 2.5$ for a variety of aspect ratios were studied. The torus is placed in a vertical stream (from down to up) of uniform flow velocity U_∞ as shown in Figure 1. The positive direction of angular velocity at the torus surface is such that the rotating surface accelerates the uniform stream on the outer ring surface due to the no-slip requirement. On the inner ring surface, the positive rotational velocity of the wall is opposed to the oncoming flow direction.

The main aim of the present research is to find a self-propelled regime of motion. The self-motion of the torus is caused by the propulsive fluid fluxes produced by the torus on its rotating boundary. The translation velocity of torus can be in the direction of inner surface motion (positive angular velocity) or in the direction of outer surface motion (negative angular velocity). It should be noted that self-motion of the body has to be considered in whole space. In this situation, the domain of the problem is time-dependent. The Navier-Stokes equations are invariant with respect to Galilean transformation and the problem of self-motion in motionless media can be reformulated by a linear change of variables in the coordinate system attached to the body, and in a way which reduces it to a problem in time-independent domain. In this case the value of the uniform stream, U_∞, which corresponds to self-motion is unknown and has to be determined from the condition that the total drag force has to be zero. The drag force acting on the torus depends on the Reynolds number Re, aspect ratio Ar, and rate of rotation α, since $C_D = C_D(Re, Ar, \alpha)$. The self-propelled flow regime corresponds to $C_D = C_D(Re, Ar, \alpha) = 0$. Let us define α_{crit} as that which produces zero drag on the torus, *i.e.* at α_{crit}, $C_D(Re, Ar, \alpha_{crit}) = 0$. It is clear that α_{crit} depends on Re and aspect ratio Ar, *i.e.* $\alpha_{crit} = \alpha_{crit}(Re, Ar)$. It is worth noting that the case $\alpha \neq \alpha_{crit}$ also has physical meaning. It can be considered as uniform flow past a torus with rotating surface or a towed torus with rotating surface in an unbounded motionless fluid.

The influence of the rotational speed α on C_D is demonstrated in Figure 3. The drag coefficient for the flow past a torus with aspect ratio $Ar = 2$ are analyzed here for the Reynolds number 40. The curve presented in Fig. 3 shows a linear decrease in C_D with increasing positive α. For the negative α drag coefficient C_D increases with increasing module of α up to $\alpha \cong 1.5$. The following increasing of $|\alpha|$ characterizes by decreasing C_D. The cases of zero drag correspond to the self motion of torus at $\alpha \approx 4.57$ and $\alpha \approx 1.61$.

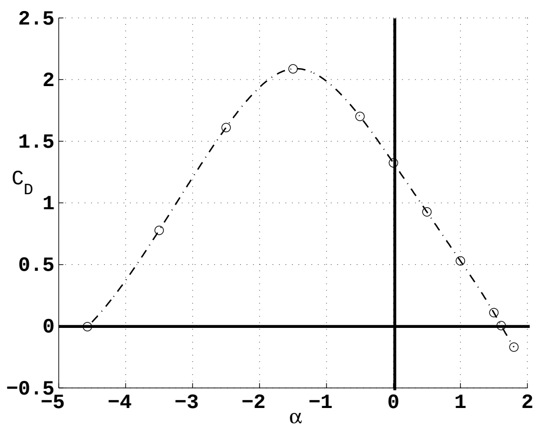

Fig. 3. Variation of drag coefficient with rate of rotation for aspect ratios $Ar = 2$ and $Re = 40$.

Figure 4 shows the stream lines patterns for $Ar = 2$, $Re = 40$ and $\alpha = -4.57$ (self-motion), -3.5, -1.5, 0.0. 1.0 and 1.61 (self motion). In the self-motion regime corresponding to the positive α, the main stream flows around the rotating toroidal fluid region which encloses the rigid torus rotating around its centerline. The torus moves in the direction of the inner surface motion as in the case of Stokes' problem.

The self-motion regime corresponding to the negative $\alpha \approx= -4.57$ associated with the jet of fluid expelled from the hole.

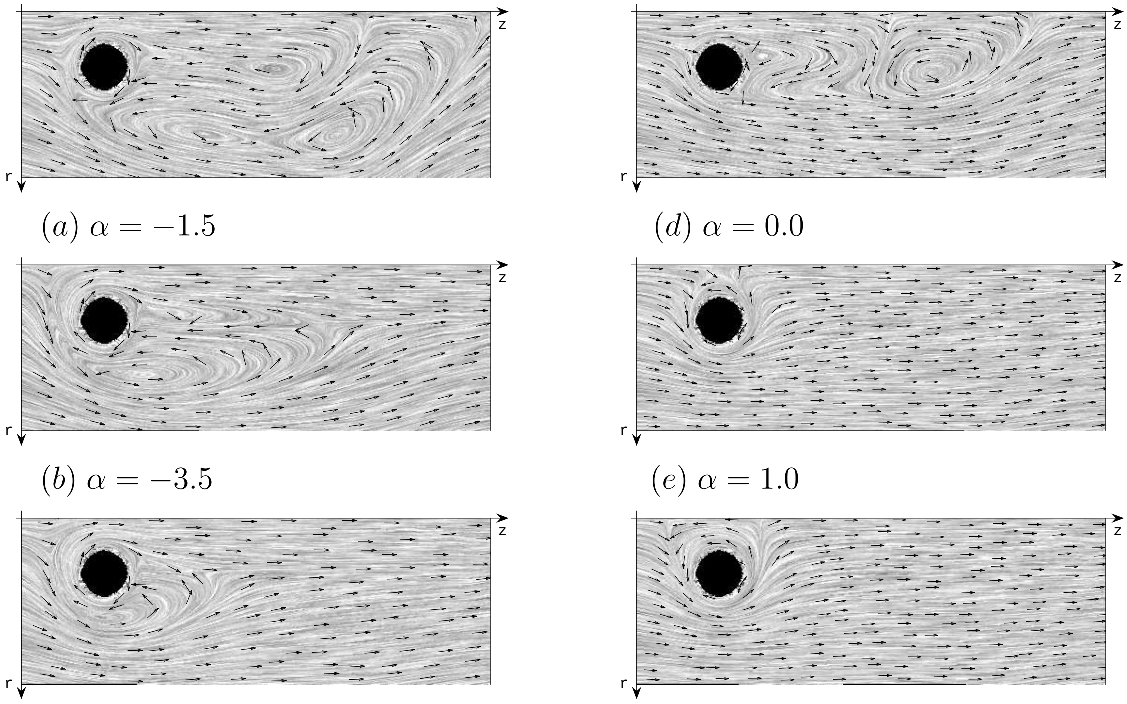

(a) $\alpha = -1.5$

(d) $\alpha = 0.0$

(b) $\alpha = -3.5$

(e) $\alpha = 1.0$

(c) $\alpha = -4.57$(self-motion: $C_D = 0$)

(f) $\alpha = 1.61$(self-motion: $C_D = 0$)

Fig. 4. Streamline patterns of flow past a rotating torus at $Re = 40$ with $Ar = 2$.

Refernces

[1] Moshkin N.P., Suwannasri P. Self-propelled motion of a torus rotating about its centerline in a viscous incompressible fluid// Phys. Fluids. 2010. vol. 22, 113602.

[2] Leshansky A.M. and Kenneth O. Surface tank treading: Propulsion of Purcell's toroidal swimmer // Phys. Fluids. 2008. vol. 20, 063104.

[3] Purcell E. M. Life at low Reynolds number// Am.J. Phys. 1997. vol. 45. p. 3–11.

[4] Thaokar R.M., Schiessel H., and Kulic, I.M. Hydrodynamics of a rotating torus// Eur. Phys. J. B. vol. 60. 2007. p. 325–336.

[5] Yanenko N.N., *The method of Fractional Steps: The Solution of Problems of Mathematical Physics in Several Variables* (New York, Springer-Verlag, 1971).